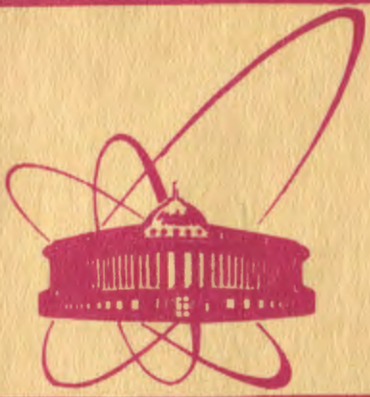

объединенный
институт
ядерных
исследований
дубна

12/1-81

112/2-81

E1-80-598

A STUDY OF PION PRODUCTION IN 4.5 GeV/c PER NUCLEON ^{4}He INTERACTIONS WITH NUCLEAR TARGETS

SKM-200 Collaboration

1980

A.U.Abdurakhimov, M.Kh.Anikina, V.S.Butsev, E.A.Dementiev,
N.S.Glagoleva, A.I.Golokhvastov, L.A.Goncharova, A.G.Grachov,
S.V.Kadykova, N.I.Kaminsky, S.A.Khorozov, E.S.Kuznetsova,
J.Lukstins, L.S.Lyubimova, A.T.Matyushin, V.T.Matyushin,
M.G.Mescheryakov, Zh.Zh.Musulmanbekov, E.O.Okonov.
T.G.Ostanevich, E.A.Shevchenko, G.L.Vardenga,
V.D.Volodin, M.S.Zhuravleva.

Joint Institute for Nuclear Research, Dubna, USSR.

L.D.Chikovani, M.G.Dzhaoshvili, L.L.Gabuniya,
E.Sh.Ioramashvili, A.A.Ivanova, E.S.Mailian, L.A.Razdolskaya.

Institute of Physics, Georgian SSR Academy of Sciences,
Tbilisi, USSR.

L.V.Chkhaidze, T.D.Iobava, I.I.Tuliani.

Institute of High Energy Physics, Tbilisi State University,
Tbilisi, USSR.

M.Gazdzicki, R.Szwed, E.Skrzypczak, J.A.Zakrzewski.

Institute of Experimental Physics, University of Warsaw,
Warsaw, Poland.

E.K.Khusainov, N.N.Nurgozhin.

Institute of High Energy Physics, Kazakh SSR Academy
of Sciences, Alma-Ata, USSR.

Y.S.Pol, G.G.Taran.

Lebedev Physical Institute of the Academy of Sciences,
Moscow, USSR.

E1-80-598

A STUDY OF PION PRODUCTION IN 4.5 GeV/c PER NUCLEON ^{4}He INTERACTIONS WITH NUCLEAR TARGETS

SKM-200 Collaboration

Submitted to "Nuclear Physics".

1. INTRODUCTION

During the last few years, pion production processes in nucleus-nucleus interactions at relativistic energies have been studied in several experiments using various detection techniques[1-5].

In this paper we present the results of an analysis of ^{4}He interactions, at a momentum of 4.5 GeV/c per incident nucleon, with pure Li , C , Al , Cu and Pb targets obtained using the 2m streamer chamber. The experimental setup allowed us to register all charged secondaries in 4π geometry, thus making it possible to study pion production in various subsets of events, e.g., differing in the degree of projectile fragmentation. In fact, the number of nucleons registered among projectile charged fragments can be used as a measure of the impact parameter. This possibility of a quasi-exclusive study of nucleus-nucleus interactions with a distinction between central and peripheral collisions is rather essential for testing various theoretical approaches to the problem of nucleus-nucleus interactions.

In this work we are interested in the production of negative secondaries (mostly π^--mesons) since their samples are free from a contamination with fragments of the projectile and target nucleus. In section 2 the experimental conditions are briefly described, whereas in section 3 are discussed the data on projectile fragmentation processes and the problem of fragment identification. Various characteristics of negative secondaries such as multiplicities, transverse momenta and rapidities are presented in section 4. The discussion of the experimental results and their comparison with predictions of some theoretical models are given in section 5.

2. EXPERIMENTAL SETUP

The experimental setup consisted of the 2 m streamer chamber, placed in a magnetic field of 0.8 T, and a system of counters (see Fig.1, also[6,14]). The streamer chamber (200x100x60 sm^3) used as a detector was filled with a pure

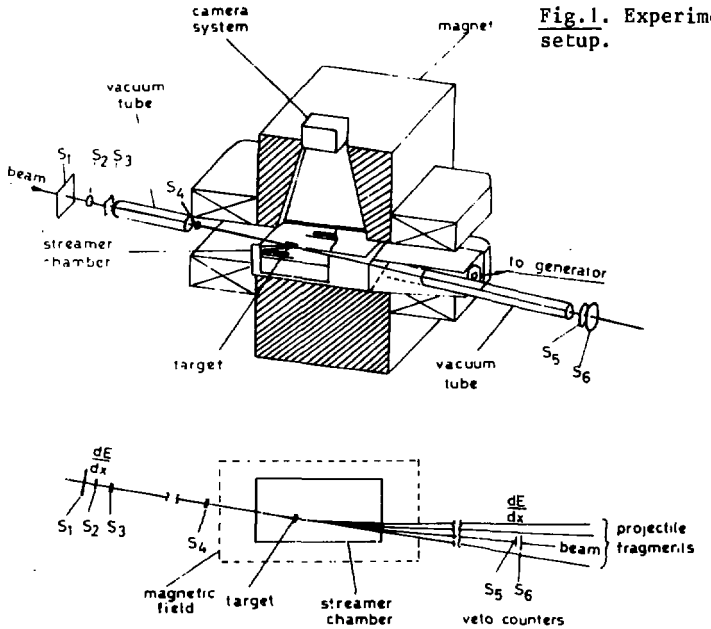

Fig.1. Experimental setup.

neon gas at atmospheric pressure and exposed to a beam of ^{4}He nuclei accelerated at the Dubna synchrophasotron up to a momentum of 4.5 GeV/c per incident nucleon. The chamber was triggered by a beam telescope and a veto-counter system. The latter covered a rather small solid angle (0.6 msr for the Li target and 0.2 msr for the heavier ones).

The targets made in the form of thin discs were mounted inside the fiducial volume of the chamber. Two photographs were taken for each event with a stereophotocamera placed above the chamber.

The charges, $Z = 1$ or $Z = 2$, of fast secondary particles were determined by visual examination of ionization on their tracks. All negative π^--mesons with momenta larger than 40 MeV/c (60 MeV/c in the case of the Li target which was much thicker than the other targets, see Table 1) were

Table 1

Number of measured events and typical values of measurement errors

Targets	Number of measured events	Target thickness g/cm^2	Typical values of errors		
			momentum		
			projectile fragments*	pions	emission angle
Li	4024	1.59	3 - 9 %		
C	2151	0.40			
Al	933	0.41	5 - 16 %	4 %	5 mr
Cu	590	0.47			
Pb	233	0.23	**		

* The errors in momentum determination increase with the fragment mass.

** Projectile fragments were not measured; the analysis was limited to distinguishing between "central" events and those with at least one charged fragment.

registered and subsequently measured. Geometrical reconstruction of the measured events was then performed.

The numbers of measured events and typical values of errors in momentum and angular measurements are given in Table 1.

It should be noted that some corrections have to be applied to the primary data because of the following effects:

a) The triggering system bias: some events, for which the projectile fragment hit the veto-counter system (see Fig.1) and thus simulated the ^{4}He particle passing through the system, were lost in our detection setup. The analysis of the geometry of the whole setup and of the angular (e.g., azimuthal angle) distributions and momentum characteristics of the observed fragments allows one to evaluate correction factors for the "lost" events (about (16 $\pm$ 4)% events for the Li and (0 $\pm$ 4)% for the C , Al and Cu targets).

b) Some negative secondaries could not be measured and/or could not be geometrically reconstructed because of their unfavourable geometry or because of flares in the streamer

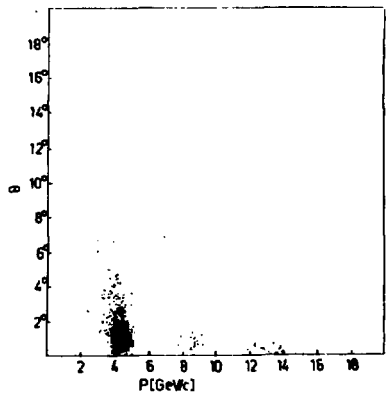

Fig.2. A plot of emission angles, θ , against momenta, p , for positive relativistic secondaries (Z = 1) in ^{4}He-Li interactions.

chamber. Fortunately, the measurement losses of π^- -mesons concerned only some well defined intervals of emission angles and, consequently, appropriate corrections based on the azimuthal symmetry could be introduced. The fraction of π^- -mesons, lost for measurements and subsequently corrected for, amounted, on the average, to about 10%.

c) The corrections for one-prong events, which could have escaped detection, were also taken into account. In most cases the corrections were (2 - 4)%.

Other sources of experimental biases, namely: i) a contamination of the sample of negative secondaries with an admixture of electrons, ii) secondary interactions in the target, were also analyzed and corrected for (for details see [4b]).

3. PROJECTILE FRAGMENTATION

In most cases projectile (stripping) fragments consisting of two or more nucleons can be identified by their momentum (close to $p_{inc}/4 \cdot A_{fr}$) and angular characteristics (strong forward collimation). In the case of stripping protons, however, their identification is much less clear. When dealing with a sample of singly charged relativistic positive secondaries, one has to remember that such a sample includes not only the protons stripped from the incident nucleus but also the projectile protons, which have undergone rescattering or inelastic interaction with the target nucleus, and knock-on fragments of the target nucleus. As an example, figure 2 presents the combined angular-momentum characteristics of singly charged relativistic positive secondaries for the Li target.

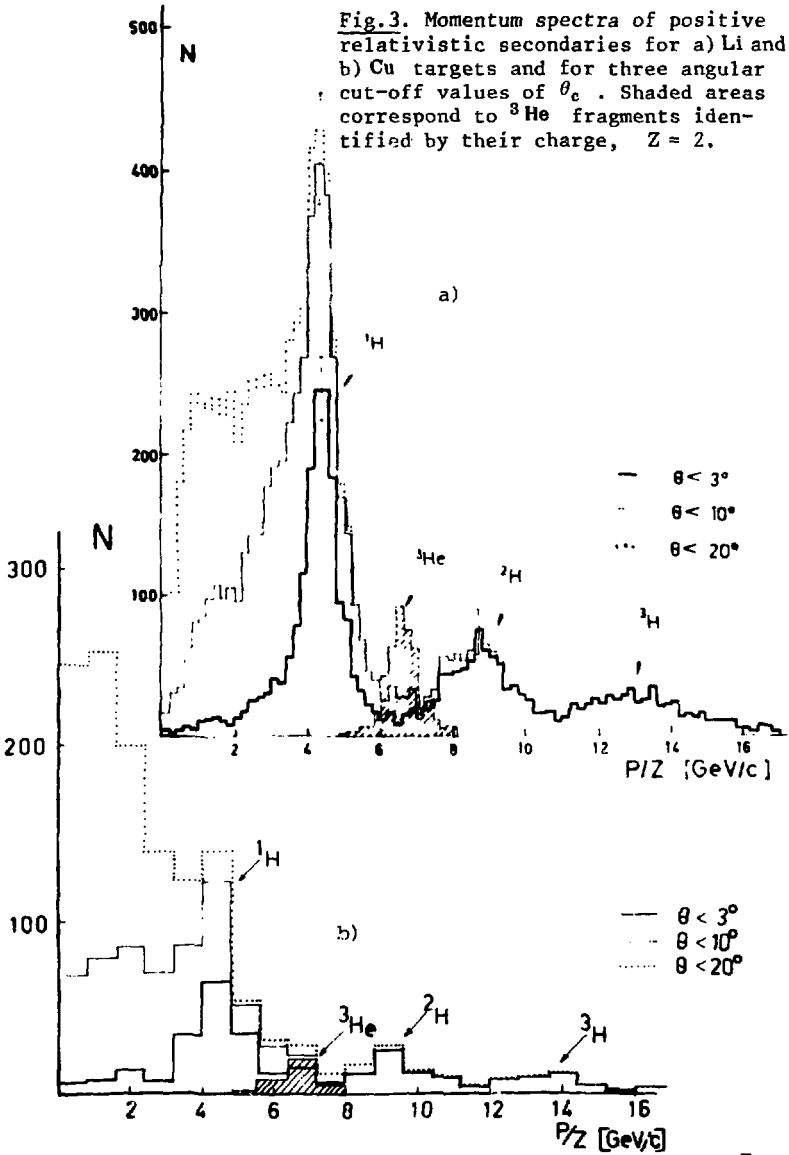

Fig.3. Momentum spectra of positive relativistic secondaries for a) Li and b) Cu targets and for three angular cut-off values of θ_c . Shaded areas correspond to ^{3}He fragments identified by their charge, Z = 2.

Figure 3 shows the momentum spectra of positive secondaries emitted at angles $\theta \leq \theta_c$ for three cut-off values of θ_c = 3°, 10° and 20° for the Li and Cu targets. In the case of the Li target a better separation of various fragments of the projectile is due both to several times richer statistics and to lower measurement errors (Table 1).

Using the angular and momentum characteristics presented in Figs.2 and 3, one cannot determine well defined momentum and angular intervals for fragmentation protons. Therefore any experimental definition of fragmentation protons involves some unavoidable arbitrariness. Whenever only the yield of fragments of each kind had been required (e.g., for the determination of inclusive cross sections), a statistical method of estimation of fragments was used, namely the momentum distributions were fitted by Gaussian curves*, and hence the numbers of fragments in the overlapping regions were obtained. Whenever the identification of individual tracks had been required, the following definitions (derived from Figs.2 and 3) of the projectile fragments were used.

i) ^1H , Z = 1, emission angle $\theta \leq 5°$,
2.5 GeV/c $\leq p <$ 6.5 GeV/c.

ii) ^2H , Z = 1, emission angle $\theta \leq 5°$,
6.5 GeV/c $\leq p <$ 10.8 GeV/c.

iii) ^3H, Z = 1, emission angle $\theta \leq 5°$,
10.8 GeV/c $\leq p <$ 20 GeV/c.

iv) ^3He , Z = 2, emission angle $\theta \leq 5°$,
5 GeV/c $\leq p <$ 8 GeV/c.

Cross sections for various fragmentation processes have been obtained, and the results are given in Table 2.

Inclusive cross sections are shown in the upper part of Table 2. The cross sections presented in the fifth row of Table 2 (σ periph) correspond to the sum of fragmentation channels in which at least two nucleons in the stripping fragments have been observed. The events with $N \geq 2$ nucleons registered in the stripping will be hereafter referred to as "peripheral" events corresponding to large impact parameter values. The last row of Table 2 gives the cross sections for interactions in which no charged fragments of the projectile have been observed. These events will be hereafter referred

---

* An angular cut-off at 5° was used for protons (heavier fragments are much more collimated).

Table 2

Cross section values for fragmentation processes (mb)

Fragmentation process		Targets				α
		Li	C	Al	Cu	$(\sigma \sim A_T^{\alpha})$
inclusive emission of the projectile fragments	^1H	166±13	227±20	319±34	417±45	0.40±0.05
	^2H	84±15	91±27	113±38	159±45	0.27±0.14
	^3H	47±5	58±9	73±20	95±14	0.30±0.08
	^3He	48±5	49±8	70±15	95±20	0.30±0.10
"peripheral" events		208±20	244±26	313±48	412±70	0.29±0.08
"central" events		51±5	106±10	248±28	525±50	1.01±0.06

to as "central"* events (small impact parameter values). All cross sections are normalized to σ^{inel} [74b,8]. The errors given in Table 2 include statistical errors, errors of σ^{inel} values, uncertainties due to the corrections (section 2) and, in the case of σ^{centr} and σ^{periph}, those due to shifting (within resonable limits) of the momentum intervals in the above definition of the projectile fragments. The observed dependence of σ on the target mass number, A_T, (Table 2) is consistent, within rather large errors, with $\sigma \sim A_T^{\alpha}$. The

* One should keep in mind that in this experiment the neutrons, stripped from the incident nucleus, have not been registered, and, consequently, our "central" collision samples are not identical with samples of qenuinely central events defined as those in which no fragments of the incident nucleus are registered in a narrow forward cone. Nevertheless, the "centrality" and "peripherality" signatures used in this experiment enable us to correlate pion characteristics with low and large average impact parameter values.

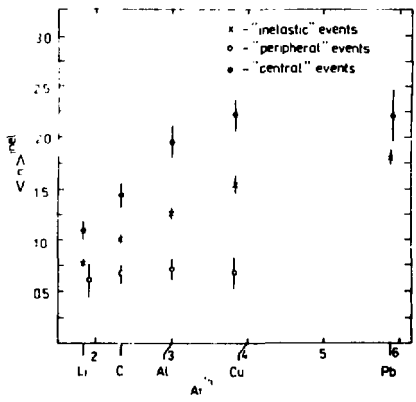

Fig.4. Dependence of the average multiplicity of negative pions on the target mass number, A_T, for all inelastic events and separately for the samples of "central" and "peripheral" interactions.

best fit value of the parameter α is close to 0.3 for all fragmentation channels in which charged fragments of the projectile are observed, whereas the A_T dependence of the cross section is much stronger ($\alpha \approx 1$) for "central" events.

4. PION PRODUCTION

Our experimental data allow us to analyse negative pion production separately for "peripheral" and "central" events (as defined in the preceding section). Samples of all inelastic events, averaged over the impact parameter, will be hereafter called "inelastic" collisions.

Figure 4 presents the data on the average multiplicity of π^- -mesons, $\langle n \rangle^{inel}$, as a function of the target mass number, A_T. The index "inel" in the symbol $\langle n \rangle^{inel}$ shows that the data are normalized to σ^{inel}. A marked dependence is seen of $\langle n \rangle^{inel}$ on A_T for "central" events and for total samples of inelastic events, whereas no significant dependence of $\langle n \rangle^{inel}$ on A_T is observed.

Figure 5 shows the rapidity distributions $\frac{dn}{dy} = \frac{1}{\sigma^{inel}} \cdot \frac{d\sigma(\pi^-)}{dy}$ of negative pions for all nuclear targets (rapidity y in the laboratory system is $y = \frac{1}{2} \ln \frac{E+p_L}{E-p_L}$). There is no A_T dependence of the rapidity distribution for the $Y > 2$ region while a well marked dependence of dn/dY on A_T is seen for the $Y < 2$ region. A quantitative illustration of this effect is shown in Fig.6.

The A_T dependence of the average multiplicity is somewhat stronger (the value of α fitted to the $\langle n \rangle \sim A_T^{\alpha}$ dependence is ~ 0.5) for pions with low rapidity $Y < 0$ (target

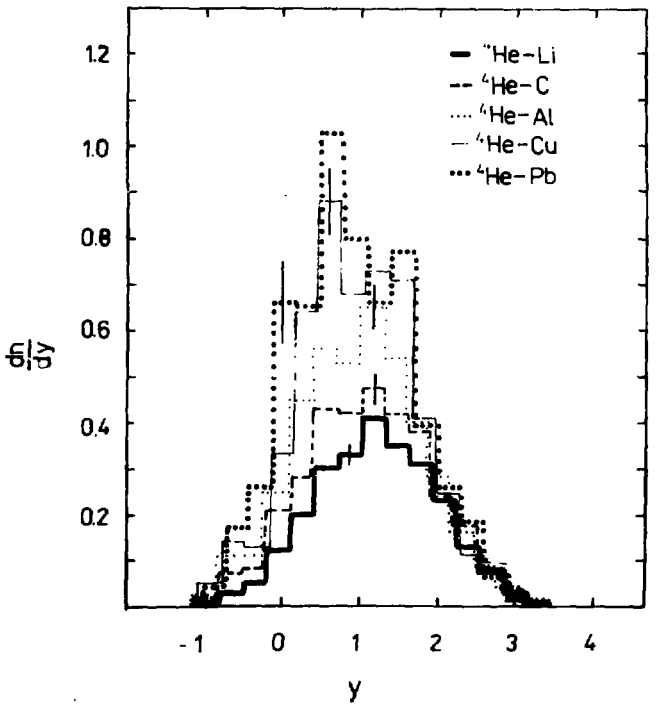

Fig.5. Rapidity distribution, dn/dy , for negative pions from ^{4}He interactions with Li , C , Al , Cu and Pb target nuclei.

fragmentation region) than for pions emitted with rapidities $0 \leq Y \leq 2.28$ ($\alpha \approx 0.3$). The π^- -multiplicity in the high rapidity region, $Y > 2.28$ (projectile fragmentation) seems to be independent of the target mass number ($\alpha \approx 0$).

The behaviour of the average rapidity, $\langle Y \rangle$, as a function of A_T is shown in Fig.7a,b,c for various subsets of negative π^- -mesons.

The decrease of $\langle Y \rangle$ with increasing A_T for

i) pions from "peripheral" events (Fig.7a),
ii) pions from events with multiplicities of negative pions $n \leq 2$ (Fig.7b) and

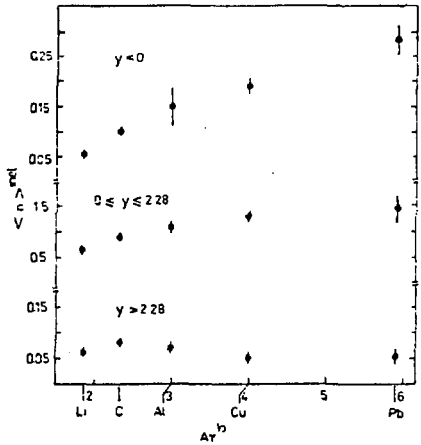

Fig.6. Dependence of the average multiplicity of negative pions on the target mass number for three rapidity regions: $Y < 0$, $0 \leq Y \leq 2.28$ and $Y > 2.28$.

iii) pions with transverse momenta $p_T \geq 0.4$ GeV/c (Fig.7c) is significantly weaker than the decrease of $\langle Y \rangle$ observed for

i) pions from "central" events (Fig.7a),

ii) pions from events with $n > 2$ (Fig.7b) and

iii) pions with $p_T \leq 0.2$ GeV/c (Fig.7c).

The dependence of $\langle Y \rangle$ for total samples of "inelastic" events is also shown in Fig.7a for comparison with the behaviour of $\langle Y \rangle$ vs A_T for various subsets of pions.

Figure 8 presents the transverse momentum distribution of negative pions ($\frac{dn}{dp_T} = \frac{1}{\sigma^{inel}} \cdot \frac{d\sigma(\pi^-)}{dp_T}$).

The average multiplicities for the two regions of transverse momentum values of p_T ($p_T \leq 0.2$ GeV/c, $p_T \geq 0.4$ GeV/c) are plotted against A_T in Fig.9. The A_T dependence of n^{inel} is stronger for low p_T pions than for those with higher transverse momenta.

The behaviour of the average transverse momentum, $\langle p_T \rangle$, as a function of A_T is presented in Fig.10. The $\langle p_T \rangle$ dependence on the target mass number, A_T, is similar for pions emitted from "all inelastic" and from "central" events ($\langle p_T \rangle$ decreases with increasing A_T). For pions emitted from "peripheral" events $\langle p_T \rangle$ seems to be independent of A_T, at least within the precision and scope of data available at present.

For π^--mesons produced in the events with $n \leq 2$ (Fig.10b) the $\langle p_T \rangle$ values are higher than for π^--mesons produced in the events with $n > 2$ (Fig.10b).

It is also seen (Fig.10c) that $\langle p_T \rangle$ in the central region of rapidities is much larger than $\langle p_T \rangle$ of pions with rapidities $Y < 0$ or $Y > 2.28$.

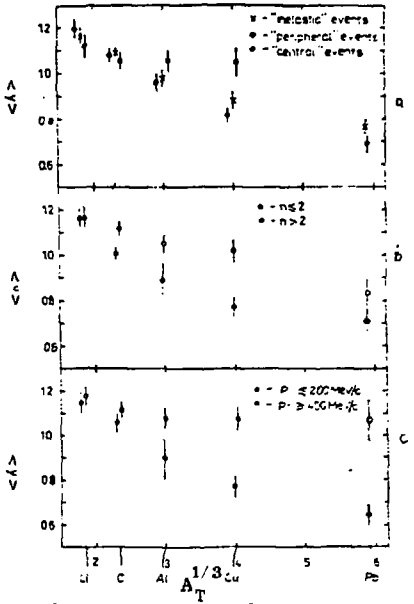

Fig.7. A_T dependence of the average rapidity values Y for a) all "inelastic", "peripheral" and "central" events, b) low ($n \leq 2$) and high ($n > 2$) multiplicity events and c) pions with high ($p_T \geq 0.4$ GeV/c) and low ($p_T \leq 0.2$ GeV/c) transverse momenta.

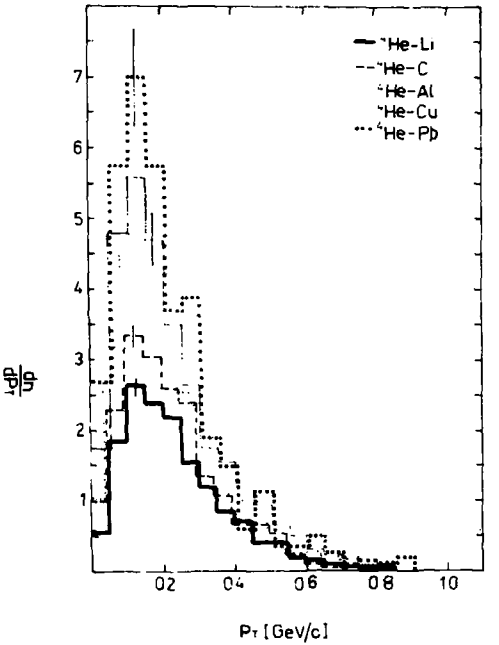

Fig.8. Transverse momentum distributions for negative pions emitted from inelastic interactions of ^4He with Li , C , Al , Cu and Pb nuclear targets.

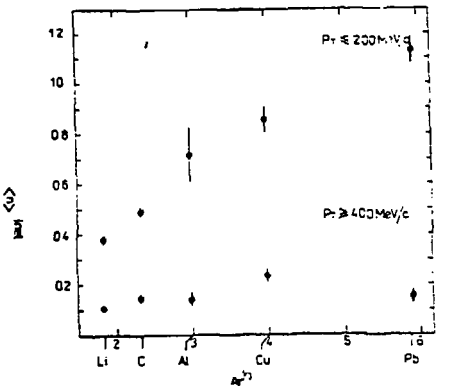

Fig.9. Dependence of the average multiplicity of negative pions on the target mass number for *pions with high* ($p_T \geq 0.4$ GeV/c) and low ($p_T \leq 0.2$ GeV/c) transverse momenta.

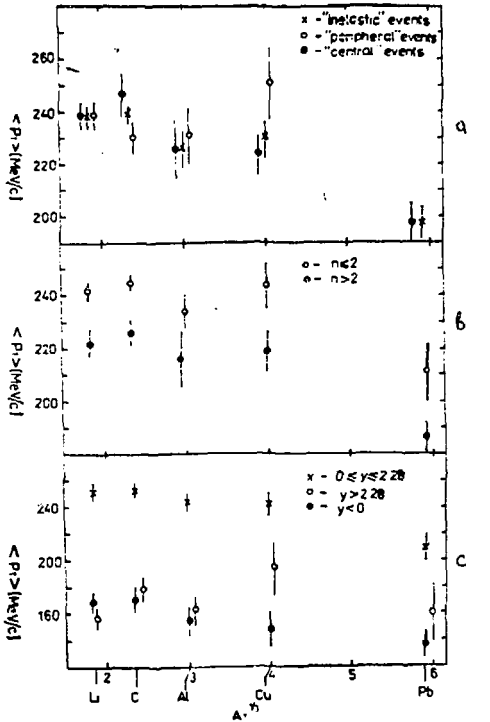

Fig.10. A_T dependence of the transverse momentum of negative pions for a) all "inelastic", "peripheral" and "central" events, b) low ($n \leq 2$) and high ($n > 2$) multiplicity events and c) pions with low ($Y < 0$), intermediate ($0 \leq Y \leq 2.28$) and high ($Y > 2.28$) rapidity values.

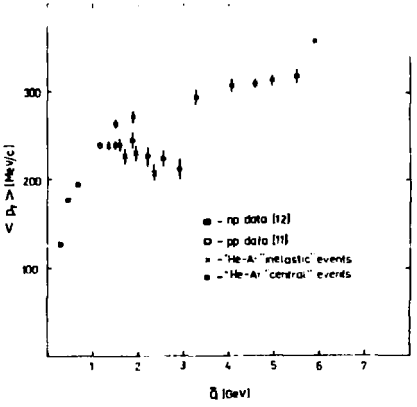

Fig.11. Dependence of average transverse momenta, $\langle p_T \rangle$, on the average available energy of collision, Q (see text).

5. DISCUSSION AND CONCLUSIONS

The experimental material analysed in this paper comprises

i) data on multiplicity, n, angular and momentum distributions (rapidity, Y, transverse momentum, p_T) for negative π^- - mesons emitted from individual acts of inelastic interactions of ^4He with nuclei of the five targets covering a wide range of mass number (A_T) values and

ii) data on projectile charged fragments observed in these interactions. The latter information has yielded the signature for "central" (small impact parameter b) and "peripheral" (large b) collisions. Main experimental results can be summarized as follows:

1) Cross sections for various fragmentation channels are consistent with an A_T dependence of the form $\sigma \sim A_T^{\alpha}$, where $\alpha \approx 1$ for "central" interactions, whereas $\alpha \approx 1/3$ for "peripheral" ones.

2) In "peripheral" collisions no significant A_T dependence is observed of the average multiplicity $\langle n \rangle$, rapidly $\langle Y \rangle$ and transverse momentum $\langle p_T \rangle$ of negative pions.

In "central" collisions a marked increase of $\langle n \rangle$ and a decrease of $\langle Y \rangle$ and $\langle p_T \rangle$ with increasing A_T is observed.

3) Among several other correlations between n, Y and p_T values presented in section 4 the A_T dependence of $\langle Y \rangle$ is

a) weak and qualitatively similar for "peripheral" and low multiplicity ($n \leq 2$) events as well as for pions with high transverse momenta ($p_T \geq 0.4$ GeV/c) and

b) much stronger and qualitatively similar for both "central" and high multiplicity ($n > 2$) events as well as for pions with low transverse momenta ($p_T \leq 0.2$ GeV/c).

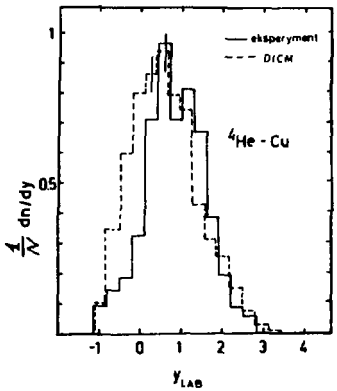

Fig.12. Rapidity distribution for ^{4}He–Cu inelastic interactions obtained in this experiment and predicted by DICM for the same incident momentum.

Our experimental data on transverse momenta of negative pions were further analyzed in order to test the validity of the so-called "minimal version" of CTM based on the "universality assumption" of nucleon-nucleon and tube-tube collisions [10]. Figure 11 shows the dependence of $\langle p_T \rangle$ on $\bar{Q}$, the average available energy in the centre of mass of colliding objects. In nucleon-nucleon interactions the colliding objects are nucleons themselves, while in nucleus-nucleus interactions the colliding objects are "tubes" (coherent tube model, CTM). For nucleus-nucleus collisions the $\bar{Q}$ values were obtained by averaging the available collision energy over various tubes and various impact parameters involved in the interactions.

The black points and open circles in Fig.11 correspond to pp and np data, respectively [11,12], while the squares correspond to the averaged p_T values of pions emitted from "inelastic" and "central" ^{4}He–A interactions plotted against $\bar{Q}$.

All $\langle p_T \rangle$ values obtained in our experiment are close to those for nucleon-nucleon interactions at 4.5 GeV/c (corresponding to $Q \approx 1.3$ GeV), whereas, according to the "minimal version" of CTM, the $\langle p_T \rangle$ should be very close both for nucleus-nucleus and NN interactions at equal $\bar{Q}$ values.

We conclude that our experimental data are not consistent with predictions derived from the "minimal version" of CTM (see also [14] for discussion of the A_T dependence of $\langle n \rangle$ in inelastic nucleus-nucleus collisions). It should be noted that our conclusion is intensitive to the details of calculation of the $\bar{Q}$ values.

Predictions of an "independent collision" model, namely of the intranuclear cascade model (DICM [7]), are compared to

Table 3

Comparison of average rapidity values for π^- -mesons from ^{4}He–Cu collisions with predictions of DICM[7]

transverse momentum / average rapidity	$p_T \leq 0.2$ GeV/c		$p_T \geq 0.4$ GeV/c	
$\langle Y \rangle$	exp	DICM	exp	DICM
	0.86±0.04	0.56±0.02	1.04±0.06	0.90±0.04

the results of this experiment. Figure 12 shows the rapidity distribution for negative pions emitted from ^{4}He–Cu inelastic interactions. One can see a marked disagreement, particularly in the low rapidity region.

A further comparison of the DICM predictions with our experimental data concerns correlations between rapidity and transverse momentum values for negative pions from ^{4}He–Cu interactions. The experimental and predicted $\langle Y \rangle$ values are not consistent with each other (see Table 3).

As is seen from Table 3, the disagreement is mainly due to low transverse momentum pions. It should be stressed that a direct application of the cascade model to the propagation of low energy pions seems to be questionable, and it requires a more sophisticated consideration[15] . This disagreement of the DICM predictions with the experimental data (as well as the disagreements concerning pion multiplicities[14]) seems to suggest that in DICM the number of intranuclear collisions is slightly overestimated, at least in the case of heavy target nuclei.

The above observations lead to the conclusion that both CTM in its minimal version and DICM do not reproduce the experimental data, the disagreement being qualitative and, consequently, more serious in the former case.

At the present level of the predictive power of theoretical models, decisive tests of their validity are not possible in most cases. However, one should hope that the experimental material presented in this paper may serve as a basis for testing theoretical models formulated so as to yield quantitative predictions.

The authors are grateful to V.D.Toneev for close cooperation during the data analysis. We are also very thankful to the technical staffs of all collaborating laboratories for their efficient help in carrying out the exposures and for performing measurements and scanning.

REFERENCES

1. a) Otterlund I. Cosmic and Subatomic Physics Report, LUIP, 1979, 7904, and references therein;
   b) Shabratova G.S. et al. Acta Phys. Slov., 1978, 28, p.132.
2. Abdrakhmanov E.O. et al. JINR, P1-10779, Dubna, 1977; Yad. Fiz., 1978, 27, p.1020.
3. Fung S.Y. et al. Phys. Rev. Lett., 1978, 40, p.292.
4. a) Anikina M.Kh. et al. JINR, P1-10590, Dubna, 1977;
   b) Aksinenko V. et al. Nucl. Phys., 1979, A324, p.266.
5. Mayer W.G. et al. LBL-9151/79/Phys. Rev. C.
6. Abdurakhimov A.Kh. et al. JINR, 13-10692, Dubna, 1977.
7. Gudima K.K., Toneev V.D. Yad. Fiz., 1978, 27, p.295.
8. Aksinenko V. et al. JINR, E1-12713, Dubna, 1979.
9. Meng Ta-Chung. Phys. Rev. Lett., 1979, 42, p.1331.
10. Afek Y. et al. Phys. Rev. Lett., 1978, 41, p.849.
11. Complication: Rossi A. et al. Nucl. Phys., 1975, B84, p.269.
12. Abdivaliev A. et al. JINR, B1-1-12181, Dubna, 1979.
13. Bergström L., Fredriksson S. Phys. Lett., 1978, 78B, p.337.
14. Aksinenko V.D. et al. Nucl. Phys., 1980, A346, p.200.
15. Giunochio J.N., Johnson M.B. Phys. Rev., 1980, 21C, p.1056.

Received by Publishing Department
on September 5 1980.